Neurobiology of Aging 87 (2020) 35–43

Contents lists available at ScienceDirect

Neurobiology of Aging

journal homepage: www.elsevier.com/locate/neuaging

Gut microbiota manipulation through probiotics oral administration restores glucose homeostasis in a mouse model of Alzheimer's disease

Laura Bonfili*, Valentina Cecarini, Olee Gogoi, Sara Berardi, Silvia Scarpona, Mauro Angeletti, Giacomo Rossi, Anna Maria Eleuteri

School of Biosciences and Veterinary Medicine, University of Camerino, Camerino (MC), Italy

ARTICLE INFO

Article history:
Received 13 February 2019
Received in revised form 4 November 2019
Accepted 4 November 2019
Available online 11 November 2019

Keywords:
Alzheimer's disease
Probiotics
Glucose metabolism
AGEs

ABSTRACT

Cerebral glucose homeostasis deregulation has a role in the pathogenesis and the progression of Alzheimer's disease (AD). Current therapies delay symptoms without definitively curing AD. We have previously shown that probiotics counteract AD progression in 3xTg-AD mice modifying gut microbiota and inducing energy metabolism and glycolysis-gluconeogenesis. Ameliorated cognition is based on higher neuroprotective gut hormones concentrations, reduced amyloid-β burden, and restored proteolytic pathways. Here, we demonstrate that probiotics oral administration improves glucose uptake in 3xTg-AD mice by restoring the brain expression levels of key glucose transporters (GLUT3, GLUT1) and insulin-like growth factor receptor β, in accordance with the diminished phosphorylation of adenosine monophosphate–activated protein kinase and protein-kinase B (Akt). In parallel, phosphorylated tau aggregates decrease in treated mice. Probiotics counteract the time-dependent increase of glycated hemoglobin and the accumulation of advanced glycation end products in AD mice, consistently with memory improvement. Collectively, our data elucidate the mechanism through which gut microbiota manipulation ameliorates impaired glucose metabolism in AD, finally delaying the disease progression.

1. Introduction

Glucose uptake and metabolism are impaired in the brain of Alzheimer's disease (AD) subjects and strongly contribute to the pathogenesis and the progression of the disease and to the manifestation of clinical signs (Gardener et al., 2016). Under physiological conditions, the brain largely depends on glucose for energy production (Chen and Zhong, 2013). An adequate supply of glucose from the blood stream depends on glucose transporters (GLUTs) (Scheepers et al., 2004). In mammalian brain, GLUT1 and GLUT3 prevalently transport glucose from blood into the extracellular space (Qutub and Hunt, 2005). Reduced expression levels of GLUT1 and GLUT3 in the cerebral cortex of AD subjects impaired brain glucose uptake, leading to hyperphosphorylation of tau protein, which is a major pathological hallmark of AD (Bloom, 2014). Some authors propose gene therapy to enrich glucose transporters content in selected brain areas to ameliorate glucose uptake and proteostasis dysfunction in AD (Duran-Aniotz and Hetz, 2016).

Glucose uptake is also influenced by functional abnormalities of critical metabolic sensors, including adenosine monophosphate-activated protein kinase (AMPK) and protein kinase B, also named Akt, with consequent energy metabolic impairment and severe implications in AD pathology (Rickle et al., 2004). Amyloid-β (Aβ) oligomers transiently reduce AMPK and Akt phosphorylation causing neuronal metabolic defects (Rickle et al., 2004). In the brain, AMPK acts as a regulator of cellular energy homeostasis. AMPK activity increases during glucose deprivation, metabolic stress, ischemia, and hypoxia in neurons both in vivo and in vitro (Weisova et al., 2009). Specifically, in case of reduced intracellular energy levels, AMPK phosphorylates metabolic enzymes and regulates gene expression of GLUTs. In addition, metabolic stresses activate AMPK and the enzyme functionality depends on hormones and cytokines affecting whole-body energy balance. Interestingly, AMPK can directly phosphorylate tau and activated/phosphorylated AMPK has been observed in tauopathies and AD brains (Vingtdeux et al., 2011).

* Corresponding author at: School of Biosciences and Veterinary Medicine, University of Camerino, Via Gentile III da Varano, 62032 Camerino (MC), Italy. Tel: +39 0737 403247; fax: +39 0737 403290.
E-mail address: laura.bonfili@unicam.it (L. Bonfili).

0197-4580/
https://doi.org/10.1016/j.neurobiolaging.2019.11.004

Similarly, Akt activity is upregulated in AD, concomitant with neurofibrillary aggregates (Rickle et al., 2004). Akt plays a highly conserved role in the regulation of cellular energy metabolism. It regulates phosphatidylinositol-3-kinase survival signaling for insulin-like growth factor I (IGF-I) and other trophic factors; it phosphorylates tau and influences the production and deposition of Aβ (Bhat and Budd, 2002).

Deterioration of insulin signaling strongly contributes to brain metabolic impairments in AD. For example, IGF-I promotes Aβ clearance in the brain and reduced cerebral uptake of IGF-I results in increased Aβ levels (Carro et al., 2006). IGF-I has a role in the proteasome-mediated removal of oxidized proteins in the brain (Crowe et al., 2009). The levels of both IGF-I and its receptor significantly decrease in the hippocampus and somatosensory cortex of aged mice, causing age-related changes in the brain (Lee et al., 2014). Postmortem studies on human brain frequently show insulin resistance with reduced activation of receptors and inhibition of downstream neuronal survival and plasticity mechanisms in AD (Talbot et al., 2012).

Moreover, tau hyperphosphorylation occurs in mice having abnormal brain insulin levels (Schubert et al., 2003). An increasing number of studies correlate glucose intolerance and impairment of insulin metabolism with a higher risk of developing AD (Butterfield et al., 2014; Pardeshi et al., 2017). Elevated concentrations of glycated hemoglobin (HbA1c), which reflect the average glucose level in the blood over the past 3 months, have been associated with cognitive impairment. High fasting blood glucose levels have been linked to decreased memory in healthy elderly (Yaffe, 2007), thus representing a risk factor for AD (Velazquez et al., 2017; Xu et al., 2007). Additional studies indicate massive alterations of protein glycosylation in specific brain regions of patients with AD (Frenkel-Pinter et al., 2017).

Moreover, advanced glycation end products (AGEs), deriving from Maillard reaction between carbohydrates and proteins, increase in neurons in hippocampus of AD subjects. AGEs are involved in Aβ aggregation and accumulation, playing an important role in AD (Vitek et al., 1994).

Currently, no definitive treatment exists for AD and available therapies preserve cognition and memory and delay the loss of function. In recent years, an increasing number of studies have been focusing on the role of the gut microbiota in disorders associated with the central nervous system (CNS), with special interest in the modulation of the gut-brain axis. Modulation of gut microbiota using probiotics has been proposed for the prevention and treatment of several pathologies including CNS disorders (Hsiao et al., 2013). For example, probiotic supplementation has reversed cognitive impairment and spatial memory loss in diabetic rats (Davari et al., 2013). Interestingly, the rational manipulation of intestinal microbiota in rats treated with a probiotic mixture attenuated the age-related deficit in long-term potentiation and modulated the expression of several genes in the brain (Distrutti et al., 2014). Moreover, bacterial by-products such as short-chain fatty acids exert neuromodulatory effects and directly act on gastrointestinal cells stimulating the synthesis of hormones, such as leptin and glucagon-like peptide 1 (GLP-1) (Oleskin and Shenderov, 2016). Using a triple transgenic mouse model of AD (3xTg-AD mice), we have recently demonstrated that the oral administration of a novel formulation of lactic acid bacteria and bifidobacteria (namely SLAB51) counteracted cognitive decline, reduced Aβ aggregates and brain damages, and partially restored the impaired neuronal proteolytic pathways (Bonfili et al., 2017). In addition, SLAB51 mitigated oxidative stress in 3xTg-AD mouse brain by activating sirtuin-1 (SIRT1)-dependent mechanisms (Bonfili et al., 2018). Improvement of cognitive function was supported by enriched gut content of anti-inflammatory short-chain fatty acids and increased plasma concentrations of neuroprotective gut peptide hormones that play a role in modulating neuronal functions such as learning and memory (Bonfili et al., 2017). In detail, SLAB51 oral administration influenced energy metabolism and glycolysis-gluconeogenesis in AD mice, enhancing GLP-1 and glucose-dependent insulinotropic polypeptide (GIP) plasma concentrations (Holscher, 2014). Moreover, GIP and GLP-1 receptor agonists have been proposed as therapeutic agents in neurodegenerative disorders (Han et al., 2016).

Considering the key role of impaired cerebral glucose metabolism in cognitive dysfunction and histopathological alterations typical of AD, the amelioration of glucose uptake and metabolism represents a promising approach in AD therapy. In this perspective, the present work focused on exploring the effects of SLAB51 oral administration on glucose metabolism in 3xTg-AD mice and their wild-type (wt) counterpart. For this purpose, 8-week-old mice have been orally administered with SLAB51 for a period of 16 and 48 weeks and the brain expression levels of GLUT3, GLUT1, insulin-like growth factor-I receptor β (IGF-IRβ), the phosphorylated form of AMPK, Akt, and tau proteins have been evaluated. Plasma levels of glycated hemoglobin and AGEs brain concentration have been also monitored.

2. Materials and methods

2.1. Reagents and chemicals

SLAB51 probiotic formulation has been provided by Ormendes SA (Jouxtens-Mézery, Switzerland, https://agimixx.net). SLAB51 contains 8 different live bacterial strains: *Streptococcus thermophilus* DSM 32245, *Bifidobacterium lactis* DSM 32246, *B. lactis* DSM 32247, *Lactobacillus acidophilus* DSM 32241, *Lactobacillus helveticus* DSM 32242, *Lactobacillus paracasei* DSM 32243, *Lactobacillus plantarum* DSM 32244, and *Lactobacillus brevis* DSM 27961. The antibodies are described in Supplementary Table 1. Membranes and reagents for western blotting analyses were purchased from Merck KGaA, (Darmstadt, Germany). ELISA kit for HbA1c measurement was from MyBioSource (San Diego, CA, USA).

2.2. Animal model

AD triple-transgenic mice, B6;129-Psen1^{tm1Mpm} Tg (amyloid precursor protein [APP]Swe, tauP301L)1Lfa/J (named 3xTg-AD) and the wt B6129SF2 mice (separate line), were purchased from the Jackson Laboratory (Bar Harbor, ME, USA). 3xTg-AD mice contain 3 mutations associated with frontotemporal dementia or familial AD (APPSwe, tau MAPT P301L, and presenilin-1 M146V). This reliable model of human AD displays both plaque and tangle pathology, with Aβ intracellular immunoreactivity detectable at 3 months of age and hyperphosphorylation of tau protein occurring by 12–15 months of age (Oddo et al., 2003). Experiments were in accordance with the guidelines laid down by the European Communities Council (86/609/ECC) for the care and use of laboratory animals and with a protocol approved by the Italian Ministry of Health (518/2018-PR). Mice were housed in plastic cages (Makrolon, Covestro A.G., Filago, Italy) (4 animals per cage) in a temperature-controlled room (21 ± 5 °C) and 60% humidity on 12-hour light/dark reversed cycle (light was switched on at 8:00 p.m.) and maintained on laboratory diet (Mucedola, Italy) and water ad libitum. Appropriate measures minimized pain and discomfort in experimental animals.

2.3. Experimental design

Eight-week-old AD male mice (n = 48) were divided in 2 groups: one administered SLAB51 dissolved in water (n = 24), and the control group administered water (n = 24). Simultaneously, 48 age-matched wt mice were organized into wt control (n = 24) and wt-treated (n = 24) groups. The dosage of SLAB51 (200 billion bacteria/kg/d) was determined by application of the body surface area principle. The body weight was monitored during the treatment to ensure single-housed animals received the proper intake of the probiotic. Preliminary studies were performed to evaluate both viability and stability of the probiotic formulation on solubilization in water at 21 ± 5 °C. The percentage of vital bacteria was determined, for the entire time course of the experiment, by fluorescence microscopy, which revealed that 88% of the strains survived after 30 hours under the aforementioned conditions. Thus, probiotic drinking solution was freshly prepared every day. Eight mice per group were euthanized by CO_2 overdose at 8, 24, and 56 weeks of age, and the tissues were properly collected for both biochemical and immunohistochemical analyses. In detail, murine brains were quickly removed and placed on an ice-cold glass plate. Coronal sections were sagittally bisected: one portion was immediately frozen in liquid nitrogen and stored at −80 °C for biochemical analysis, and the other was fixed in 10% formalin for 8–10 hours, properly washed in PBS, dehydrated, and embedded in paraffin for sectioning.

2.4. Preparation of brain extracts

On sacrifice, brain was homogenized (1:5 weight/volume of buffer) in 50 mM Tris buffer, 150 mM KCl, 2 mM EDTA, pH 7.5. Homogenates were immediately centrifuged at 13,000 × g for 20 minutes at 4 °C and the supernatants were used. Protein concentration was measured with the Bradford protein assay (Bradford, 1976).

2.5. Western blotting analyses

Brain homogenates were analyzed through western blotting assays to measure the levels of GLUT3, GLUT1, IGF-IRβ, AMPK, p-AMPK, Akt, p-Akt, tau, p-tau, and AGE. In detail, for each time point, brain homogenates (30-μg total protein) were separated through SDS-PAGE on 10% or 12% gels, and electroblotted onto polyvinylidene fluoride membranes. Successively, on incubation with specific antibodies, the immunoblot detections were carried out with an enhanced chemiluminescence (ECL) western blotting analysis system. Molecular weight markers (6.5–205 kDa) were included in each gel. Glyceraldehyde-3-phosphate dehydrogenase (GAPDH) was used to check equal protein loading. The densitometric analysis has been conducted as previously described (Amici et al., 2008). Briefly, each western blot was scanned (16-bit gray scale) and the obtained digital data were processed through Image J (NIH) to calculate the background mean value and its standard deviation. The background-free image was then obtained subtracting the background intensity mean value from the original digital data. The integrated densitometric value associated with each band was then calculated as the sum of the density values over all the pixels belonging to the considered band having a density value higher than the background standard deviation. The band densitometric value was then normalized to the relative GAPDH signal intensity. The ratios of band intensities were calculated within the same western blot. All the calculations were carried out using the MATLAB environment (The MathWorks Inc, Natick, MA, USA). For AGE, both bands have been included in the analysis.

2.5.1. Immunohistochemical analysis

The effects of SLAB51 on glucose transporters GLUT3 and GLUT1 in specific brain regions were investigated immunohistochemically (IHC). Three 3 μm-thick brain sections from each animal (n = 8 per sub-group), at ∼0.84, 1.20, and 1.56 mm lateral from the midline (Paxinos and Franklin, 2001), were prepared. Selected sections were deparaffinized and rehydrated according to standard protocols and used for GLUT1, GLUT3, and p-tau immunohistochemical detection. For each time point, brain sections from treated and untreated wt and AD mice (n = 8 per subgroup) were fixed in a 50:50 mixture of methanol and acetone for 5 minutes and incubated with the specific antibody. For GLUT1 detection, brain sections were incubated overnight with anti-glucose transporter GLUT1, diluted 1:100, cross-reacting with mouse, rat, and human. For GLUT3 detection, brain sections were incubated overnight with anti-glucose transporter GLUT3, diluted 1:150, cross-reacting with mouse, rat, and human. Nonspecific binding was blocked by incubation for 10 minutes with a protein-blocking agent (Dako, Carpinteria, CA, USA) before overnight incubation with the primary antibody in a moist chamber. The immunoreaction with streptavidin–immunoperoxidase (Abcam, Cambridge, UK) was visualized with 3,3′-diaminobenzidine substrate (Vector Laboratories, Burlingame, CA, USA). Tissues were counterstained with Mayer's hematoxylin. For negative immunohistochemical controls, the primary antibodies were omitted.

In addition, fibrillar deposits of highly phosphorylated tau in brain samples were visualized immunohistochemically using the rabbit monoclonal antibody [EPR2605] to p-tau (phospho S404) diluted 1:150. The binding of the antibody was detected with the Elite kit (Vector Laboratories), and the immunoreaction was developed using 3,3′-diaminobenzidine substrate (Vector Laboratories).

Positive cells were quantified in different brain areas from 10 appropriate fields and arithmetic means were calculated for each brain region. Results are expressed as IHC-positive cells per 62,500 μm^2. For all parameters, cells on the margins of the tissue sections were not considered for evaluation to avoid inflation of positive cell numbers. Positive cells were quantified using an image-analysis system consisting of a light microscope (Carl Zeiss, Jena, Germany), attached to a Javelin JE3462 high-resolution camera and a personal computer equipped with a Coreco-Oculus OC-TCX frame grabber and high-resolution monitor. Computerized color-image analysis was performed by using Image-Pro Plus software (Media Cybernetics, Rockville, MD, USA). The entire cerebral cortex and hippocampus were separately sampled with the counting frame size 250 μm × 250 μm for cortex and 100 μm × 100 μm for hippocampus. The area of each section in all brain cross-sections in each mouse was recorded, as was the total number of neurons determined by immunostaining as previously described. For each mouse, the total brain area was calculated as the sum of the areas of all fields in all brain cross-sections on one slide. For GLUT1 and GLUT3, positive cells were counted per section, and stained cell densities were expressed as the number of cells per square millimeter of analyzed section area (Rossi et al., 2014). The area of interest in the hippocampus was CA1. p-tau immunoreactive area was measured in the threshold segmented cortical and hippocampal regions of interest and normalized to the total region of interest area. The pathologist performing quantification of amyloid burden was blind to age, treatment type, and genotype of mice.

2.6. ELISA assay for HbA1c levels determination

Glycated hemoglobin concentration was measured in plasma samples promptly supplemented with protease inhibitors (Pefabloc and TPCK) using a Mouse Glycated hemoglobin A1c ELISA Kit (MyBioSource) according to the manufacturer's instructions.

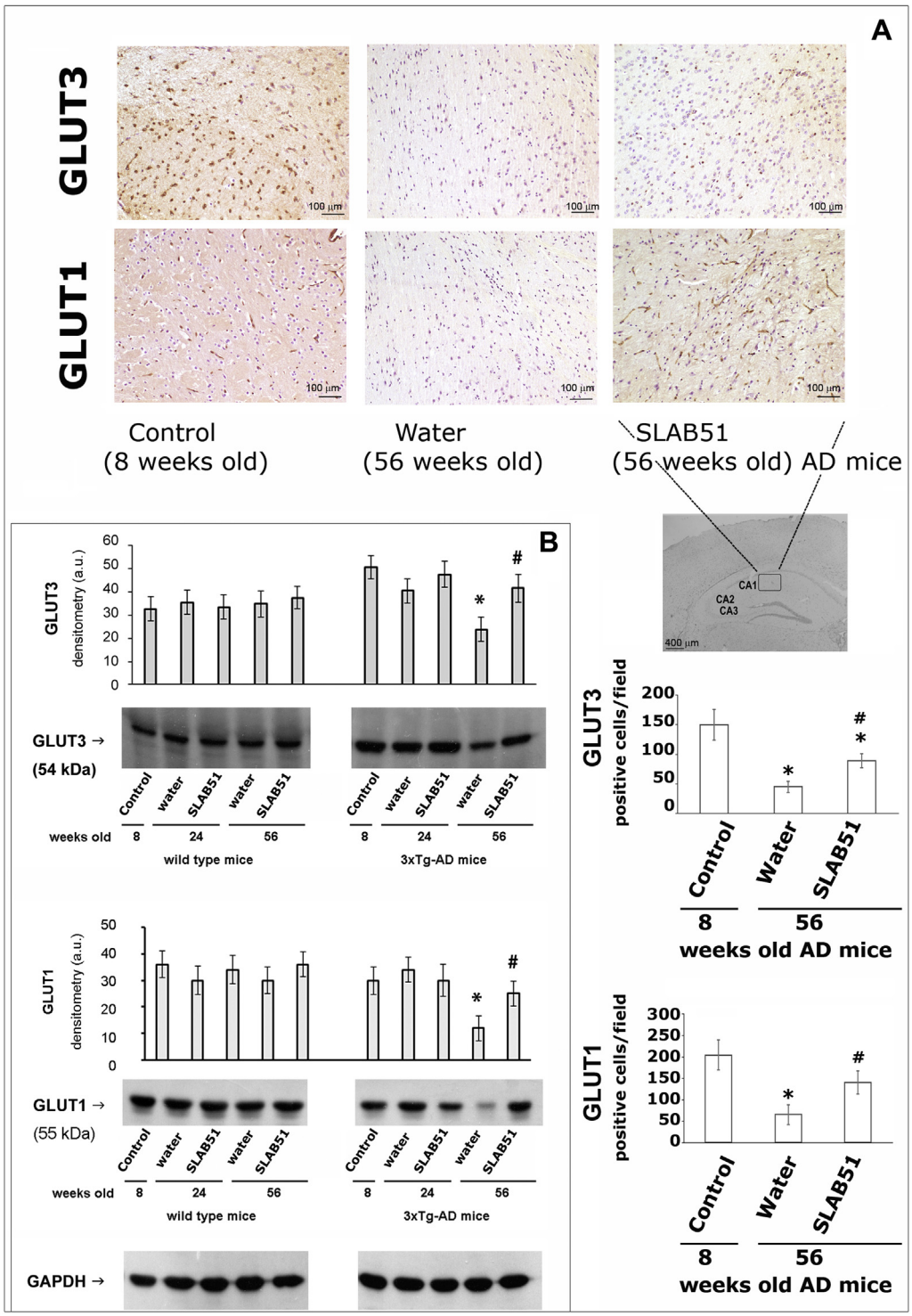

Fig. 1. Glucose transporters in the brain of wt and AD mice orally administered with SLAB51 for 16 and 48 weeks. (A): GLUTs IHC staining. Immunodetection of GLUT3 and GLUT1 proteins in brain sections of 8- and 56-week-old AD mice. Representative images of immunohistochemical staining of hippocampal area CA1 are shown (the hippocampal region of interest is indicated in the 5× image). The histograms show the GLUT3- and GLUT1-positive cells/field, respectively. (B): GLUT3 and GLUT1 brain expression levels. Representative immunoblots obtained from ECL western blotting analysis system and corresponding densitometric analyses derived from 6 separate blots are shown. Equal protein loading was verified by using an anti-GAPDH antibody. In A and B, data points marked with an asterisk are statistically significant compared with 8-week-old untreated control mice of the same genotype ($^*p < 0.05$). Data points marked with a hashtag are statistically significant compared with age-matched untreated mice ($\#p < 0.05$). Abbreviations: AD, Alzheimer's disease; ECL, enhanced chemiluminescence; GAPDH, glyceraldehyde-3-phosphate dehydrogenase; GLUT, glucose transporter; IHC, immunohistochemical.

2.7. Statistical analysis

Biochemical and IHC data are expressed as mean values ± standard error (S.E.). Statistical analysis was performed with one-way ANOVA, followed by the Bonferroni test using Sigma-Stat 3.1 software (SPSS, Chicago, IL, USA). Statistical significance of treated mice compared with untreated 8-week-old mice of the same genotype is indicated with asterisks ($^*p < 0.05$). To describe the effect

of SLAB51 treatment, statistical significance of treated mice compared with age-matched untreated mice of the same genotype is indicated with hashtags (#$p < 0.05$).

3. Results

3.1. SLAB51 oral administration influences glucose uptake in AD mice

GLUT3 and GLUT1 are the major neuronal glucose transporters. IHC analysis showed a decrease of both proteins of AD untreated mice at 56 weeks compared with 8 weeks of age, particularly in the hippocampal CA1 region (Fig. 1A), in the subgranular zone and the molecular layer of the dentate gyrus for GLUT3, and in the blood capillaries of the dentate gyrus for GLUT1 consistently with previous reports (Lee et al., 2018). Positive cells significantly increased in treated animals at 56 weeks of age relative to age-matched untreated animals. Western blotting analyses confirmed that expression levels of both GLUTs significantly decreased in untreated 56-week-old AD mice, in agreement with the impaired functionality of brain cells (Harr et al., 1995), and were restored with SLAB51 treatment (Fig. 1B), suggesting a positive effect of probiotic oral consumption on glucose uptake. No significant variations have been observed in the wt group.

Several key regulators can influence the expression level of GLUTs. Interestingly, the AMPK activity plays a central role in cellular glucose uptake, with increased activity interfering with the expression of GLUTs. In fact, AMPK has been characterized as a critical regulator of cellular function in response to energy stress within cells. Accordingly, increased levels of total AMPK were detected in aged AD mice with respect to 8-week-old mice (Fig. 2A). The phosphorylated form of AMPK, corresponding to the activated form, increased in untreated AD mice at 24 and 56 weeks of age compared with 8 weeks of age, and diminished with SLAB51 treatment in the 24- and 56-week-old mice relative to the age-matched untreated mice. No significant variations were observed in wt animals. Akt is another kinase implicated in regulating the translocation and the biosynthesis of insulin-sensitive glucose transporters in most cell types. AD mice showed an increase of the phosphorylated/activated form of Akt that was only significantly mitigated with SLAB51 treatment at 56 weeks of age. Again, no significant variations were observed in wt animals (Fig. 2B). Functional abnormalities of these critical metabolic sensors (both AMPK and Akt) cause energy metabolism impairment and correlate with tau hyperphosphorylation, which is one of the main features of AD.

3.2. Phosphorylated tau levels in SLAB51-treated mice

The extent of tau phosphorylation was evaluated using a p-tau (Ser404) antibody by western blotting and IHC. As expected, p-tau increased in untreated 24- and 56-week-old AD mice (Fig. 3). Western blotting analysis revealed a significant decrease of p-Tau levels in the brains of mice treated with SLAB51 (Fig. 3A). IHC staining of brain sections showed progressive accumulation of p-tau in the hippocampus of untreated AD mice between 8 and 56 weeks of age. The process culminated in the formation of differently sized aggregates especially in the hippocampus of 56-week-old untreated AD mice in association with some morphological evidence of hippocampal atrophy. Hyperphosphorylated tau aggregates decreased in number and size in treated animals at both 24 and 56 weeks of age (Fig. 3B).

3.3. Glycated hemoglobin plasma levels

Elevated fasting serum glucose and insulin resistance have been linked to decreased memory and AD. Considering that glycated hemoglobin is currently considered an excellent indicator of insulin resistance and a reliable retrospective index of average blood glucose level (Sherwani et al., 2016), plasma concentrations of HbA1c were measured in control and treated groups of mice.

Fig. 4 shows an age-dependent increase of HbA1c in untreated AD mice. SLAB51 attenuated the increase in HbA1c plasma concentrations, proving that this probiotic mixture positively influences glucose metabolism in AD mice.

3.4. Insulin-like growth factor-I receptor brain expression

It has been largely described that the dysregulation of blood glucose homeostasis due to increased glucose production, impaired

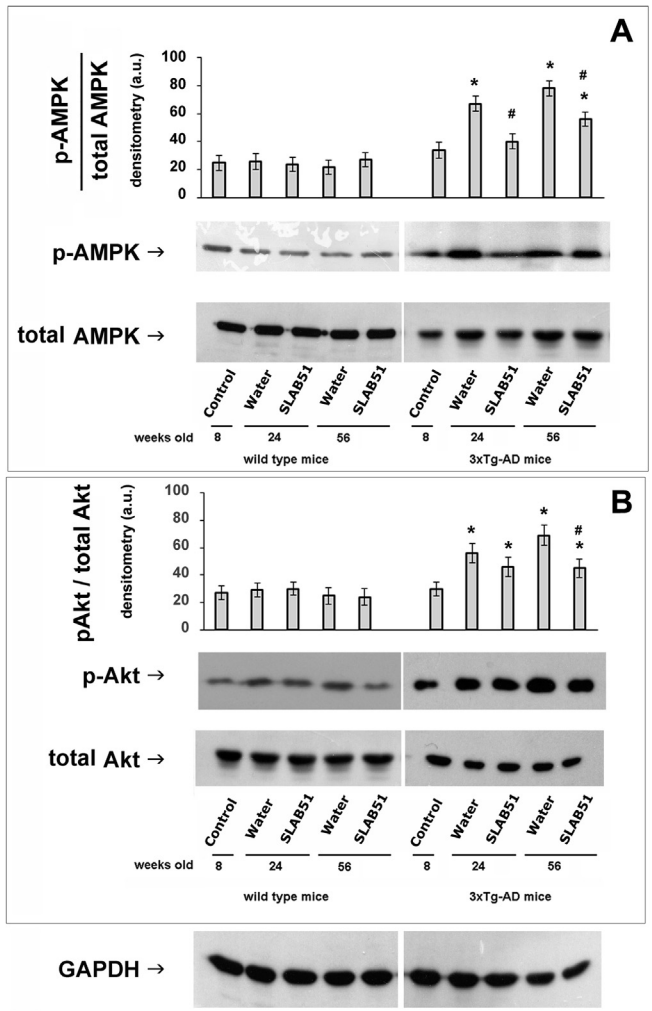

Fig. 2. Phosphorylation levels of AMPK (A) and Akt (B) in wt and AD mice orally administered with SLAB51 for 16 and 48 weeks. Representative immunoblots and the ratio of intensity of the bands for p-AMPK/total AMPK and p-Akt/total Akt are reported. Equal protein loading was verified by using an anti-GAPDH antibody. The detection was performed using an ECL western blotting analysis system. Data points marked with an asterisk are statistically significant compared to 8-week-old untreated control mice (*$p < 0.05$). Data points marked with a hashtag are statistically significant compared to age-matched untreated mice (#$p < 0.05$). Abbreviations: AD, Alzheimer's disease; AMPK, adenosine monophosphate–activated protein kinase; ECL, enhanced chemiluminescence; GAPDH, glyceraldehyde-3-phosphate dehydrogenase.

insulin production, and insulin resistance represents a risk factor for AD. Considering that IGF-I has a role in the proteasome-mediated removal of oxidized proteins in the brain acting as a promising therapeutic target in AD, the expression levels of IGF-IRβ have been measured in the brain of both wt and AD mice treated or not with SLAB51. Decreased amounts of IGF-IRβ were detected in 56-week-old 3xTg-AD mice, in agreement with previously published data (Lin et al., 2018); whereas no changes were observed in wt animals. Interestingly, the receptor concentration significantly increased in the brain of AD mice administered with SLAB51 (Fig. 5).

3.5. Advanced glycation end products in AD mice

Insulin resistance and high glucose concentration together with increased oxidative stress in AD brain contribute to the accumulation of AGEs, harmful products that have been associated with many chronic diseases. AGEs significantly increased in untreated AD mice and SLAB51 supplementation was effective in reducing their amount in both 24- and 56-week-old mice (Fig 6).

4. Discussion

Current established treatments for AD are only able to counterbalance the symptoms but they cannot prevent or stop the disorder. Recent studies are now targeting gut microbiota because of its role in regulating multiple neurochemical pathways through the gut-brain axis (Bhattacharjee and Lukiw, 2013; Wang and Kasper, 2014) and oral bacteriotherapy is becoming a recognized strategy for the prevention and treatment of several disorders, including CNS-related diseases (Distrutti et al., 2014; Douglas-Escobar et al., 2013; Duncan and Flint, 2013; Hsiao et al., 2013; Saulnier et al., 2013). We have recently demonstrated that the oral administration

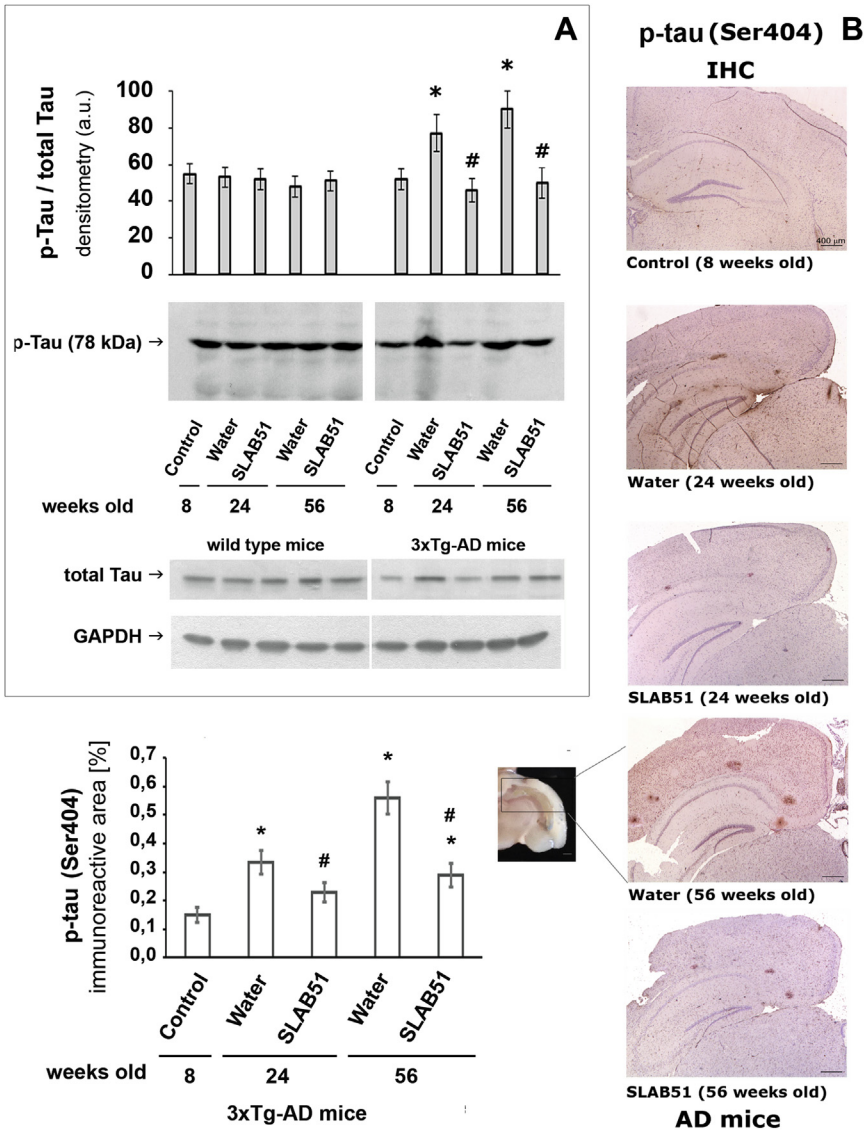

Fig. 3. Phosphorylated tau levels in wt and AD mice treated with SLAB51 for 16 and 48 weeks. (A): Representative immunoblots and the ratio of intensities of the bands p-tau/total tau are shown. Equal protein loading was verified by using an anti-GAPDH antibody. The detection was executed by an ECL western blotting analysis system. (B): p-tau (Ser404) IHC staining. Representative images of p-tau IHC staining are shown. Magnification 5x, Bars = 400 μm. The histogram shows p-tau immunoreactive area [%]. Data represent 5 sections for each brain (n = 8). In A and B, data points marked with an asterisk are statistically significant compared with 8-week-old mice (*$p < 0.05$). Data points marked with a hashtag are statistically significant compared to age-matched untreated mice (#$p < 0.05$). Abbreviations: AD, Alzheimer's disease; ECL, enhanced chemiluminescence; GAPDH, glyceraldehyde-3-phosphate dehydrogenase; IHC, immunohistochemical.

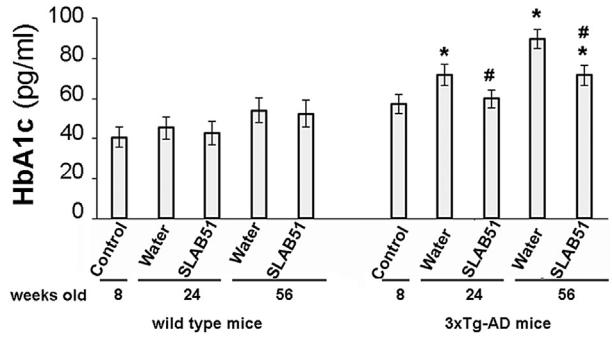

Fig. 4. Glycated hemoglobin plasma concentrations. HbA1c plasma concentration of both wt and AD mice are expressed as picograms per milliliter. Data points marked with an asterisk are statistically significant compared to 8-week-old untreated control mice (*$p < 0.05$). Data points marked with a hashtag are significantly different compared to age-matched untreated mice (#$p < 0.05$). Abbreviations: AD, Alzheimer's disease.

of SLAB51 probiotic formulation modified gut microbiota in 3xTg-AD mice, and favored several metabolic pathways associated with energy metabolism, amino acid metabolism, and nucleotide metabolism. Improvement of cognitive performances observed in these mice was supported by increased plasma concentrations of neuroprotective gut hormones and correlated with decreased Aβ load and partial recovery of neuronal proteolytic pathways with consequent delay of AD progression (Bonfili et al., 2017, 2018).

Considering that impaired cerebral glucose metabolism strongly contributes to AD onset and progression, we focused this work on the evaluation of the effects of SLAB51 oral administration on glucose uptake and metabolism using 3xTg-AD mice and the wt B6129SF2 mice. As expected, AD mice showed impaired glucose uptake compared with wt animals. In detail, levels of GLUTs decreased in the brain of aged AD animals together with the increase of phosphorylated AMPK and Akt. In fact, these kinases play a central role in glucose uptake, also influencing GLUTs' expression.

Here, we demonstrate for the first time that probiotics are able to counteract insulin resistance by restoring the brain expression level of GLUTs and diminishing the phosphorylation of key metabolic regulators such as AMPK and Akt, consequently decreasing tau phosphorylation.

Our results are consistent with previous in vivo and in vitro studies describing AMPK increased activity during glucose deprivation, metabolic stress, ischemia, and hypoxia in neurons (Weisova et al., 2009). The levels of p-AMPK and p-Akt decreased in SLAB51-treated AD mice by a similar amount, with the latter being implicated in regulating the translocation and biosynthesis of insulin-sensitive glucose transporters in most cell types. Functional abnormalities of both AMPK and Akt cause energy metabolic impairment and correlate with tau hyperphosphorylation, one of the main features of AD. It has been indicated that AMPK is a key player in the development of AD pathology because it can phosphorylate tau (Domise et al., 2016). As expected, increased tau phosphorylation was observed in 24- and 56-week-old AD mice, particularly in the hippocampus. The percentage area of phospho-tau-positive staining decreased in SLAB51-treated AD animals in accordance with the reduced levels of phosphorylated/activated AMPK and Akt (Domise et al., 2016; Vingtdeux et al., 2011) and with the partial restoration of GLUTs expression levels. These data are in line with previous studies showing that defective glucose transport determines glucose metabolism impairment, together with abnormal tau phosphorylation (Shah et al., 2012). Tau hyperphosphorylation in the hippocampus of untreated AD mice, together with the increase of pAMPK and pAkt and the decrease of GLUTs expression levels are in agreement with papers demonstrating the involvement of AMPK in AD-associated Aβ and tau pathology (Wang et al., 2019). Moreover, several studies propose that defective glucose transport leads to reduced glucose metabolism, causing abnormal tau phosphorylation (Liu et al., 2009). The increase of AMPK and Akt-mediated cerebral glucose metabolism is another

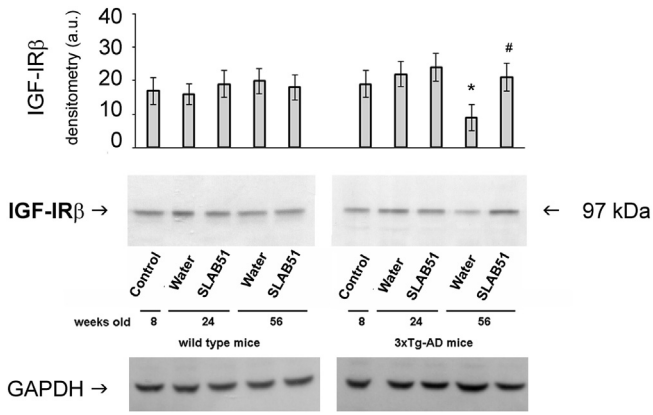

Fig. 5. IGF-IRβ levels in the brain of wt and AD mice treated with SLAB51 for 16 and 48 weeks. Representative immunoblots and corresponding densitometric analyses (expressed as arbitrary units, a.u.) obtained from 6 separate blots are shown. Anti-GAPDH antibody was used to verify equal protein loading. The detection was by an ECL western blotting analysis system. Data points marked with an asterisk are statistically significant compared with 8-week-old untreated control mice (*$p < 0.05$). Data points marked with a hashtag are significantly different compared to age-matched untreated mice (#$p < 0.05$). Abbreviations: AD, Alzheimer's disease; ECL, enhanced chemiluminescence; GAPDH, glyceraldehyde-3-phosphate dehydrogenase; IGF-IRβ, insulin-like growth factor receptor β.

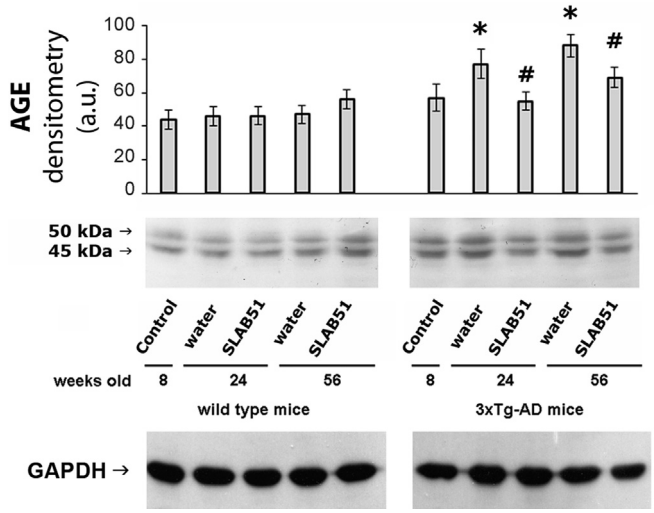

Fig. 6. AGE levels in the brain of wt and AD mice treated with SLAB51 for 16 and 48 weeks. Representative immunoblot and corresponding densitometric analysis obtained from 6 separate blots are shown. Equal protein loading was verified by using an anti-GAPDH antibody. The detection was executed by an ECL western blotting analysis system. Data points marked with an asterisk are statistically significant compared with 8-week-old untreated control mice (*$p < 0.05$). Data points marked with a hashtag are significantly different compared with age-matched untreated mice (#$p < 0.05$). Abbreviations: AD, Alzheimer's disease; AGE, advanced glycation end product; ECL, enhanced chemiluminescence; GAPDH, glyceraldehyde-3-phosphate dehydrogenase.

mechanism through which SLAB51 counteracts AD progression. In fact, besides increasing tau phosphorylation, p-AMPK is also involved in the generation and accumulation of Aβ. Therefore, such results show a connection with our previously published data that described decreased Aβ deposits in brains of SLAB51-treated AD mice (Bonfili et al., 2017) and reinforce the idea that AMPK activation has "non-neuroprotective" properties (Cai et al., 2012). Abnormal brain insulin signaling is correlated with hyperphosphorylated tau (Liu et al., 2011) and glucose intolerance and insulin resistance were described in AD mouse models (Velazquez et al., 2017). Accordingly, we detected an increase in HbA1c plasma concentration in untreated 3xTgAD mice and decreased levels with SLAB51 administration. As a reliable retrospective indicator of long-term glycemic history, the increase of HbA1c in aging and neurodegenerations inevitably suggests an impaired memory function. The ability of SLAB51 to decrease HbA1c plasma levels demonstrates a positive effect on glucose homeostasis and is correlated with the increase of gut peptide hormones, such as GLP-1 and GIP, involved in glucose metabolism, and with the enriched gut content in metabolites that improve insulin sensitivity (Bonfili et al., 2017; Tolhurst et al., 2012).

Moreover, we observed decreased brain levels of IGF-IRβ, which regulates food intake, energy metabolism, reproduction, and cognitive functions (Gasparini and Xu, 2003). The expression level of this receptor significantly increased on SLAB51 treatment with positive implications not only on glucose metabolism but in general on AD-like progression because IGF-I is involved in the proteasome-mediated proteolysis of oxidized proteins (Crowe et al., 2009). The amelioration of glucose uptake and metabolism is also consistent with the decreased formation of AGEs in treated AD mice, indicating that, by controlling glucose metabolism and favoring the clearance of oxidized species, the formation of harmful products such as AGEs can be counteracted. Collectively, these data are in perfect agreement with our previous publication showing that probiotics consumption reduced oxidative stress in 3xTg-AD mice by activating SIRT1-dependent mechanisms (Bonfili et al., 2018). Accordingly, another study shows that AGEs increase ROS production, stimulating downstream pathways related to APP processing, Aβ production, and SIRT1 (Ko et al., 2015).

Concluding, SLAB51 oral administration in 3xTg-AD mice ameliorated impaired glucose metabolism confirming the efficacy of oral bacteriotherapy in the prevention and treatment of AD. Data presented here reinforce the idea that gut microbiota modulation can influence multiple signaling pathways in the host and further contribute to the explanation of the observed ameliorated cognitive functionality in these AD mice (Bonfili et al., 2017).

Disclosure

The authors have no actual or potential conflicts of interest.

CRediT authorship contribution statement

Laura Bonfili: Methodology, Investigation, Formal analysis, Data curation, Visualization, Writing - review & editing. **Valentina Cecarini:** Formal analysis, Validation, Writing - review & editing, Investigation. **Olee Gogoi:** Investigation. **Sara Berardi:** Resources, Investigation. **Silvia Scarpona:** Resources, Investigation. **Mauro Angeletti:** Data curation, Supervision. **Giacomo Rossi:** Visualization, Supervision, Investigation. **Anna Maria Eleuteri:** Project administration, Supervision, Conceptualization.

Acknowledgements

This study was financially supported by "Noemi Avicolli" private donation to the University of Camerino.

Appendix A. Supplementary data

Supplementary data to this article can be found online at https://doi.org/10.1016/j.neurobiolaging.2019.11.004.

References

Amici, M., Bonfili, L., Spina, M., Cecarini, V., Calzuola, I., Marsili, V., Angeletti, M., Fioretti, E., Tacconi, R., Gianfranceschi, G.L., Eleuteri, A.M., 2008. Wheat sprout extract induces changes on 20S proteasomes functionality. Biochimie 90, 790–801.
Bhat, R.V., Budd, S.L., 2002. GSK3beta signalling: casting a wide net in Alzheimer's disease. Neurosignals 11, 251–261.
Bhattacharjee, S., Lukiw, W.J., 2013. Alzheimer's disease and the microbiome. Front Cell Neurosci. 7, 153.
Bloom, G.S., 2014. Amyloid-beta and tau: the trigger and bullet in Alzheimer disease pathogenesis. JAMA Neurol. 71, 505–508.
Bonfili, L., Cecarini, V., Berardi, S., Scarpona, S., Suchodolski, J.S., Nasuti, C., Fiorini, D., Boarelli, M.C., Rossi, G., Eleuteri, A.M., 2017. Microbiota modulation counteracts Alzheimer's disease progression influencing neuronal proteolysis and gut hormones plasma levels. Sci. Rep. 7, 2426.
Bonfili, L., Cecarini, V., Cuccioloni, M., Angeletti, M., Berardi, S., Scarpona, S., Rossi, G., Eleuteri, A.M., 2018. SLAB51 probiotic formulation activates SIRT1 pathway promoting antioxidant and neuroprotective effects in an AD mouse model. Mol. Neurobiol. 55, 7987–8000.
Bradford, M.M., 1976. A rapid and sensitive method for the quantitation of microgram quantities of protein utilizing the principle of protein-dye binding. Anal. Biochem. 72, 248–254.
Butterfield, D.A., Di Domenico, F., Barone, E., 2014. Elevated risk of type 2 diabetes for development of Alzheimer disease: a key role for oxidative stress in brain. Biochim. Biophys. Acta 1842, 1693–1706.
Cai, Z., Yan, L.J., Li, K., Quazi, S.H., Zhao, B., 2012. Roles of AMP-activated protein kinase in Alzheimer's disease. Neuromolecular Med. 14, 1–14.
Carro, E., Trejo, J.L., Spuch, C., Bohl, D., Heard, J.M., Torres-Aleman, I., 2006. Blockade of the insulin-like growth factor I receptor in the choroid plexus originates Alzheimer's-like neuropathology in rodents: new cues into the human disease? Neurobiol. Aging 27, 1618–1631.
Chen, Z., Zhong, C., 2013. Decoding Alzheimer's disease from perturbed cerebral glucose metabolism: implications for diagnostic and therapeutic strategies. Prog. Neurobiol. 108, 21–43.
Crowe, E., Sell, C., Thomas, J.D., Johannes, G.J., Torres, C., 2009. Activation of proteasome by insulin-like growth factor-I may enhance clearance of oxidized proteins in the brain. Mech. Ageing Dev. 130, 793–800.
Davari, S., Talaei, S.A., Alaei, H., Salami, M., 2013. Probiotics treatment improves diabetes-induced impairment of synaptic activity and cognitive function: behavioral and electrophysiological proofs for microbiome-gut-brain axis. Neuroscience 240, 287–296.
Distrutti, E., O'Reilly, J.A., McDonald, C., Cipriani, S., Renga, B., Lynch, M.A., Fiorucci, S., 2014. Modulation of intestinal microbiota by the probiotic VSL#3 resets brain gene expression and ameliorates the age-related deficit in LTP. PLoS One 9, e106503.
Domise, M., Didier, S., Marinangeli, C., Zhao, H., Chandakkar, P., Buee, L., Viollet, B., Davies, P., Marambaud, P., Vingtdeux, V., 2016. AMP-activated protein kinase modulates tau phosphorylation and tau pathology in vivo. Sci. Rep. 6, 26758.
Douglas-Escobar, M., Elliott, E., Neu, J., 2013. Effect of intestinal microbial ecology on the developing brain. JAMA Pediatr. 167, 374–379.
Duncan, S.H., Flint, H.J., 2013. Probiotics and prebiotics and health in ageing populations. Maturitas 75, 44–50.
Duran-Aniotz, C., Hetz, C., 2016. Glucose metabolism: a sweet relief of Alzheimer's disease. Curr. Biol. 26, R806–R809.
Frenkel-Pinter, M., Shmueli, M.D., Raz, C., Yanku, M., Zilberzwige, S., Gazit, E., Segal, D., 2017. Interplay between protein glycosylation pathways in Alzheimer's disease. Sci. Adv. 3, e1601576.
Gardener, S.L., Sohrabi, H.R., Shen, K.K., Rainey-Smith, S.R., Weinborn, M., Bates, K.A., Shah, T., Foster, J.K., Lenzo, N., Salvado, O., Laske, C., Laws, S.M., Taddei, K., Verdile, G., Martins, R.N., 2016. Cerebral glucose metabolism is associated with verbal but not visual memory performance in community-dwelling older adults. J. Alzheimers Dis. 52, 661–672.
Gasparini, L., Xu, H., 2003. Potential roles of insulin and IGF-1 in Alzheimer's disease. Trends Neurosci. 26, 404–406.
Han, L., Holscher, C., Xue, G.F., Li, G., Li, D., 2016. A novel dual-glucagon-like peptide-1 and glucose-dependent insulinotropic polypeptide receptor agonist is neuroprotective in transient focal cerebral ischemia in the rat. Neuroreport 27, 23–32.

Harr, S.D., Simonian, N.A., Hyman, B.T., 1995. Functional alterations in Alzheimer's disease: decreased glucose transporter 3 immunoreactivity in the perforant pathway terminal zone. J. Neuropathol. Exp. Neurol. 54, 38–41.
Holscher, C., 2014. The incretin hormones glucagonlike peptide 1 and glucose-dependent insulinotropic polypeptide are neuroprotective in mouse models of Alzheimer's disease. Alzheimers Dement. 10 (1 Suppl), S47–S54.
Hsiao, E.Y., McBride, S.W., Hsien, S., Sharon, G., Hyde, E.R., McCue, T., Codelli, J.A., Chow, J., Reisman, S.E., Petrosino, J.F., Patterson, P.H., Mazmanian, S.K., 2013. Microbiota modulate behavioral and physiological abnormalities associated with neurodevelopmental disorders. Cell 155, 1451–1463.
Ko, S.Y., Ko, H.A., Chu, K.H., Shieh, T.M., Chi, T.C., Chen, H.I., Chang, W.C., Chang, S.S., 2015. The possible mechanism of advanced glycation end products (AGEs) for Alzheimer's disease. PLoS One 10, e0143345.
Lee, C.H., Ahn, J.H., Park, J.H., Yan, B.C., Kim, I.H., Lee, D.H., Cho, J.H., Chen, B.H., Lee, J.C., Cho, J.H., Lee, Y.L., Won, M.H., Kang, I.J., 2014. Decreased insulin-like growth factor-I and its receptor expression in the hippocampus and somatosensory cortex of the aged mouse. Neurochem. Res. 39, 770–776.
Lee, K.Y., Yoo, D.Y., Jung, H.Y., Baek, L., Lee, H., Kwon, H.J., Chung, J.Y., Kang, S.H., Kim, D.W., Hwang, I.K., Choi, J.H., 2018. Decrease in glucose transporter 1 levels and translocation of glucose transporter 3 in the dentate gyrus of C57BL/6 mice and gerbils with aging. Lab. Anim. Res. 34, 58–64.
Lin, K.H., Chiu, C.H., Kuo, W.W., Ju, D.T., Shen, C.Y., Chen, R.J., Lin, C.C., Viswanadha, V.P., Liu, J.S., Huang, R.S., Huang, C.Y., 2018. The preventive effects of edible folic acid on cardiomyocyte apoptosis and survival in early onset triple-transgenic Alzheimer's disease model mice. Environ. Toxicol. 33, 83–92.
Liu, F., Shi, J., Tanimukai, H., Gu, J., Gu, J., Grundke-Iqbal, I., Iqbal, K., Gong, C.X., 2009. Reduced O-GlcNAcylation links lower brain glucose metabolism and tau pathology in Alzheimer's disease. Brain 132 (Pt 7), 1820–1832.
Liu, Y., Liu, F., Grundke-Iqbal, I., Iqbal, K., Gong, C.X., 2011. Deficient brain insulin signalling pathway in Alzheimer's disease and diabetes. J. Pathol. 225, 54–62.
Oddo, S., Caccamo, A., Shepherd, J.D., Murphy, M.P., Golde, T.E., Kayed, R., Metherate, R., Mattson, M.P., Akbari, Y., LaFerla, F.M., 2003. Triple-transgenic model of Alzheimer's disease with plaques and tangles: intracellular Abeta and synaptic dysfunction. Neuron 39, 409–421.
Oleskin, A.V., Shenderov, B.A., 2016. Neuromodulatory effects and targets of the SCFAs and gasotransmitters produced by the human symbiotic microbiota. Microb. Ecol. Health Dis. 27, 30971.
Pardeshi, R., Bolshette, N., Gadhave, K., Ahire, A., Ahmed, S., Cassano, T., Gupta, V.B., Lahkar, M., 2017. Insulin signaling: an opportunistic target to minify the risk of Alzheimer's disease. Psychoneuroendocrinology 83, 159–171.
Paxinos, G., Franklin, K.B.J., 2001. The Mouse Brain in Stereotaxic Coordinates. In: Paxinos and Franklin's The Mouse Brain in Stereotaxic Coordinates. Academic Press, San Diego.
Qutub, A.A., Hunt, C.A., 2005. Glucose transport to the brain: a systems model. Brain Res. Brain Res. Rev. 49, 595–617.
Rickle, A., Bogdanovic, N., Volkman, I., Winblad, B., Ravid, R., Cowburn, R.F., 2004. Akt activity in Alzheimer's disease and other neurodegenerative disorders. Neuroreport 15, 955–959.
Rossi, G., Pengo, G., Caldin, M., Palumbo Piccionello, A., Steiner, J.M., Cohen, N.D., Jergens, A.E., Suchodolski, J.S., 2014. Comparison of microbiological, histological, and immunomodulatory parameters in response to treatment with either combination therapy with prednisone and metronidazole or probiotic VSL#3 strains in dogs with idiopathic inflammatory bowel disease. PLoS One 9, e94699.
Saulnier, D.M., Ringel, Y., Heyman, M.B., Foster, J.A., Bercik, P., Shulman, R.J., Versalovic, J., Verdu, E.F., Dinan, T.G., Hecht, G., Guarner, F., 2013. The intestinal microbiome, probiotics and prebiotics in neurogastroenterology. Gut Microbes 4, 17–27.
Scheepers, A., Joost, H.G., Schurmann, A., 2004. The glucose transporter families SGLT and GLUT: molecular basis of normal and aberrant function. JPEN J. Parenter. Enteral Nutr. 28, 364–371.
Schubert, M., Brazil, D.P., Burks, D.J., Kushner, J.A., Ye, J., Flint, C.L., Farhang-Fallah, J., Dikkes, P., Warot, X.M., Rio, C., Corfas, G., White, M.F., 2003. Insulin receptor substrate-2 deficiency impairs brain growth and promotes tau phosphorylation. J. Neurosci. 23, 7084–7092.
Shah, K., Desilva, S., Abbruscato, T., 2012. The role of glucose transporters in brain disease: diabetes and Alzheimer's Disease. Int. J. Mol. Sci. 13, 12629–12655.
Sherwani, S.I., Khan, H.A., Ekhzaimy, A., Masood, A., Sakharkar, M.K., 2016. Significance of HbA1c test in diagnosis and prognosis of diabetic patients. Biomark. Insights 11, 95–104.
Talbot, K., Wang, H.Y., Kazi, H., Han, L.Y., Bakshi, K.P., Stucky, A., Fuino, R.L., Kawaguchi, K.R., Samoyedny, A.J., Wilson, R.S., Arvanitakis, Z., Schneider, J.A., Wolf, B.A., Bennett, D.A., Trojanowski, J.Q., Arnold, S.E., 2012. Demonstrated brain insulin resistance in Alzheimer's disease patients is associated with IGF-1 resistance, IRS-1 dysregulation, and cognitive decline. J. Clin. Invest. 122, 1316–1338.
Tolhurst, G., Heffron, H., Lam, Y.S., Parker, H.E., Habib, A.M., Diakogiannaki, E., Cameron, J., Grosse, J., Reimann, F., Gribble, F.M., 2012. Short-chain fatty acids stimulate glucagon-like peptide-1 secretion via the G-protein-coupled receptor FFAR2. Diabetes 61, 364–371.
Velazquez, R., Tran, A., Ishimwe, E., Denner, L., Dave, N., Oddo, S., Dineley, K.T., 2017. Central insulin dysregulation and energy dyshomeostasis in two mouse models of Alzheimer's disease. Neurobiol. Aging 58, 1–13.
Vingtdeux, V., Davies, P., Dickson, D.W., Marambaud, P., 2011. AMPK is abnormally activated in tangle- and pre-tangle-bearing neurons in Alzheimer's disease and other tauopathies. Acta Neuropathol. 121, 337–349.
Vitek, M.P., Bhattacharya, K., Glendening, J.M., Stopa, E., Vlassara, H., Bucala, R., Manogue, K., Cerami, A., 1994. Advanced glycation end products contribute to amyloidosis in Alzheimer disease. Proc. Natl. Acad. Sci. U. S. A. 91, 4766–4770.
Wang, X., Zimmermann, H.R., Ma, T., 2019. Therapeutic potential of AMP-activated protein kinase in Alzheimer's disease. J. Alzheimers Dis. 68, 33–38.
Wang, Y., Kasper, L.H., 2014. The role of microbiome in central nervous system disorders. Brain Behav. Immun. 38, 1–12.
Weisova, P., Concannon, C.G., Devocelle, M., Prehn, J.H., Ward, M.W., 2009. Regulation of glucose transporter 3 surface expression by the AMP-activated protein kinase mediates tolerance to glutamate excitation in neurons. J. Neurosci. 29, 2997–3008.
Xu, W., Qiu, C., Winblad, B., Fratiglioni, L., 2007. The effect of borderline diabetes on the risk of dementia and Alzheimer's disease. Diabetes 56, 211–216.
Yaffe, K., 2007. Metabolic syndrome and cognitive disorders: is the sum greater than its parts? Alzheimer Dis. Assoc. Disord. 21, 167–171.